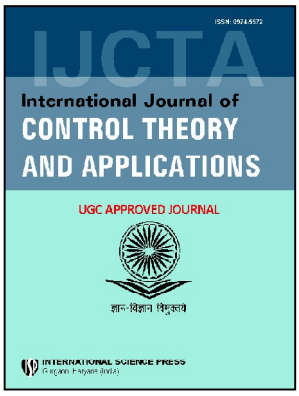

International Journal of Control Theory and Applications

ISSN : 0974-5572

Volume 10 • Number 34 • 2017

Advanced Numerical MPPT Approach for an Energy-storage Photovoltaic System Under Unbalanced Climatic Conditions

Abdessattar Jendoubi, Najib Fnaiech and Faouzi Bacha

LISI, INSAT, University of Carthage, Tunisia
E-mails: Jendoubiabdessattar@gmail.com; Fneichnejib@yahoo.fr; Faouzi.Bacha@esstt.rnu.tn

Abstract: In order to optimize a battery-storage photovoltaic system, a continuously exploit the maximum power which can be generated by the photovoltaic generator under different meteorological conditions is necessary. This exploitation overcomes the problem of mismatching between the photovoltaic generator and the load (battery), which their characteristics are nonlinear. In this paper, we present optimum system storage of energy from a photovoltaic generator to a battery. This transfer is ensured by two main compartments used in this energy-storage photovoltaic system: The first one isthe MPPT digital approach where we use the least squares method and the polynomial interpolation method. The second is the adaptator of power based on an average model of a DC/DC buck converter, which is employed to overcome the long-term simulation problem and the effects of states of charge of battery.The high performance and the effectiveness of this average model DC/DC converter and also this new numerical control method are simulated through the Matlab Simulink software, in order to best optimization of automatic charging system during a real irradiation day.

Keywords: Average model DC-DC buck converter, Least squares method, Polynomial interpolation method, Lead acid battery.

1. INTRODUCTION

The reduction of greenhouse effect, generated by fossil fuels, motivates many scientists to have recourse the renewable energies not polluting. Among these energies one finds this photovoltaic (PV) whose electrical energy is produced by PV panels [1, 4, 12].

However, two principal constraints constrain the operation of these systems. The first is the solar cell conversion efficiency which does not exceed of the received energy.The second concern the critical interactions between the sources and load (batteries) which are nonlinear. This nonlinearity is caused by the instability of irradiation along a day because of variable weather conditions andalso the nonlinearity of the characteristic of electrochemical storage battery [3].

In the literature a few results concerning the interaction between the photovoltaic sources and loads as well as the optimization of the photovoltaic energy storage system are developed. Particularly, in [6] the author has

treated the solar array as a current source; it has tracked the maximum power points to optimize the operation of the system. The principle of energy conservation was used in this work and it was implemented in a digital signal processor. The experimental results showed an excellent performance but he hasn't developed a battery model able to have a real dynamics of energy storage system.In paper [7], the author focused on the control of battery charging evolution without considering the effects of irradiation instability on the dynamic operation of the system.

This research will be divided into three axes. Firstly, the effects of the irradiation on the performance of the power solar generation are developed. Secondly, tow new numerical methods where used in this research to improve the impact of unbalanced climatic conditions on the dynamic behavior of the system. At a first step we maintain a constant temperature and variable irradiation; in this case we used the digital least square method. In second step both temperature and irradiation are variables, in this case we used the multivariateinterpolation polynomial witch based on Lagrange's numerical method. A comparative studies between these both numerical methods where developed. Thirstily, we discuss the topology of the power interface used in order to transfer of the power generated by photovoltaic array to the battery along a day. Also the dynamic battery model will be offers (Electrochemical load).

Finally, the simulations results during a real day describe the behaviour of our energy-storage photovoltaic system under unbalanced climatic conditions

2. DESCRIPTION AND MODELING OF THE BATTERY STORAGE PHOTOVOLTAIC SYSTEM

In this research, the battery-storage photovoltaic system is composed by these following subsystems:

- A PVG constituted with solar cells in series
- Variable controller of tracking power point maximal (MPPT)
- DC/DC converter
- Battery model

However, this system is given by Fig. 1

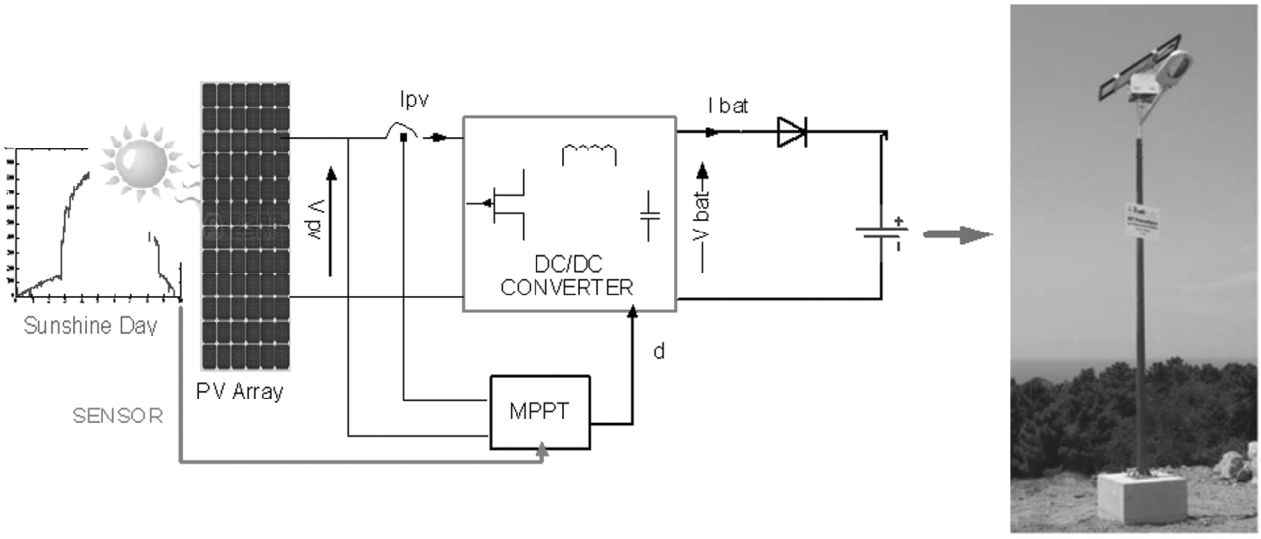

Figure 1: Diagram of the photovoltaic battery-storage system

These following sections detailed the modeling and characteristics of each subsystem of battery-storage photovoltaic system.

2.1. Photovoltaic Generator Modeling

The electrical model and parameters of solar cell are illustrated in Fig 2. This model is simulated using Matlab-Simulink Software.

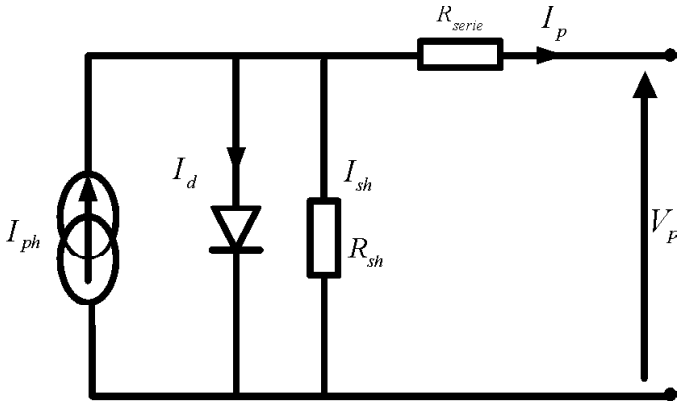

Figure 2 : Photovoltaic cell equivalent circuit

The relationship between the PV cell output current and voltage is given by equation 1.

$$I_p = I_{ph} - I_s\left[\exp\left(\frac{V_p + R_{serie} I_p}{V_T}\right) - 1\right] - \left(\frac{V_p + R_{serie} I_p}{R_{sh}}\right) \quad (1)$$

Where *Ip* and *Vp* is the output current and output voltage of a solar cell, respectively, *Iph* is the generated current under a given irradiation;is the reverse saturation current of the diode, $Vp = n * Kb * T/q$ is the thermodynamic potential of the cell.

Where *q* is the charge of an electron; *K* is the Boltzmann's constant; *n* is the ideality factor for a p-n junction; T is the temperature of a solar cell (°*K*).

Conceptually, photovoltaic cells are grouped together in order to form solar array. The relationship between the PV array output current and voltage is given by equation 2.

$$I_{pv} = N_p\ I_{ph} - N_p\ I_s\left\{\exp\left[\frac{q}{n\ K\ T}\left(\frac{V_{pv}}{N_s} + \frac{I_{pv}\ R_s}{N_p}\right)\right] - 1\right\} - \frac{N_p}{R_{sh}}\left(\frac{V_{pv}}{N_s} + \frac{I_{pv}\ R_s}{N_p}\right) \quad (2)$$

Where $Lpv = Np * Ip$ is current delivered by the cells of parallel generators; is the voltage produced across the photovoltaic generator composed toseries cells.

In the following table are shown the characteristics of PV panel brand used in our work.

Table 1
Photovoltaic Module Parametres

P_{opt} = 135 Wc	I_{opt} = 7,39A	V_{opt} = 17,6V
V_{CO} = 21,9V	I_{CC} = 8,02 A	N_s = 72 Cells

Fig 3 shows the effect of the illumination on characteristic *Vpv = f (Ppv)* of our photovoltaic generator

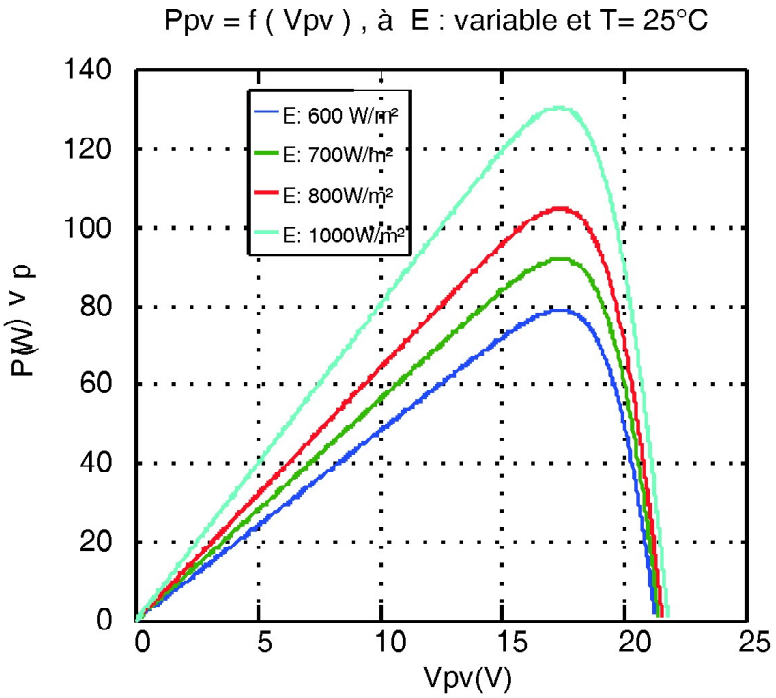

Figure 3: Variation of the GPV power and voltage, for different values of the illumination at fixed temperature

2.2. Maximum Power Point Tracking Algorithms

Bothvariables, voltage and current of the photovoltaic generator can represent the maximum power point (MPP). The photovoltaic voltage is a preferable control variable because [8]:

- The temperature range variation of the photovoltaic cell is very limited
- The irradiation variation significantly affect the photovoltaic cell current, however this irradiation doesn't have impact on voltage cell.

Many maximum power point tracking techniques for photovoltaic system have been developed to maximize the produced energy and a lot of these are well established in the literature. Starting with simple techniques as the perturbation and observation (P&O) technique or the incremental conductance, Recently, FLC has been introduced in the tracking of the MPP.They have the advantage of being robust and relatively simple to design and also they do not require a complete knowledge of the operation photovoltaic system by any designers [9].

These recommended numericalMPPT controls used in this research are developed on the following sections.

2.2.1. Least Squares Mppt Method

The least squares method is used to simulate our system at constant temperatureand variable irradiation.The variation of the irradiation during a day is illustrated by the following figure.

Forparticular irradiation points, we have determined the values of maximum powers, as well the corresponding optimum voltages of the GPV. These values are illustrated in the following table.

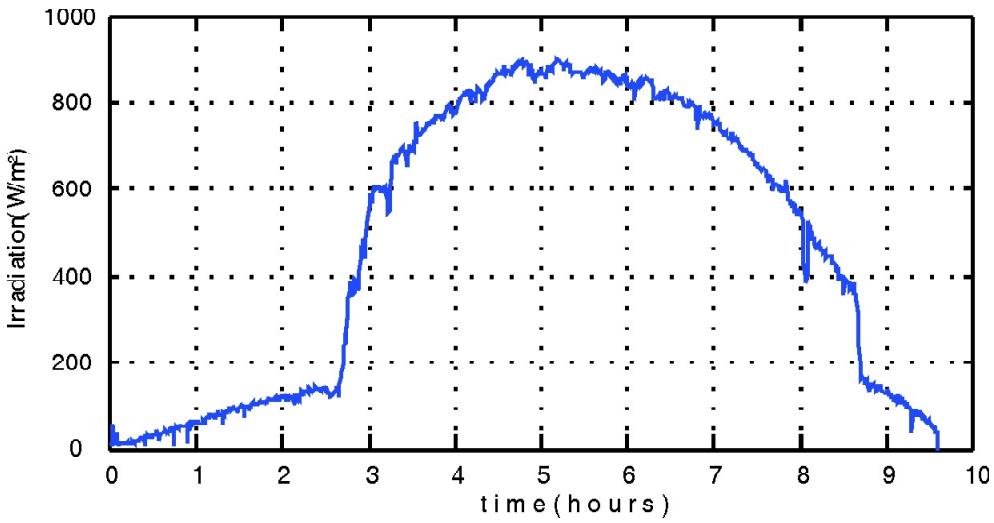

Figure 4: Variation of the illumination during a day in Tunis (Tunisia) on 05 April 2012 [1, 12]

Table 2
Parametres of Generator to Particularirradiations

Irradiation (W/m²)	*Voltage of the GPV (V)*	*Max Power of the GPV (W)*
1000	18.58	135
980	18.61	134
950	18.51	129.6
900	18.46	122.2
850	18.29	114.9
800	18.37	107.5
750	18.3	100.3
700	17.99	93.03
650	18.12	85.73
600	17.84	78.68
550	17.67	71.58
500	17.49	64.53
450	17.43	57.53
400	17.32	50.59
350	17.32	43.74
300	17.09	36.97
250	16.55	30.29
200	16.25	23.73
150	16.01	17.29
100	15.18	11.08
50	14.3	5.15

The following equations which manage the least squares MPPT approach are given as follows

$$d_{opt} = \sum_{k=0}^{n} c_k \, E_{opt} \, k \tag{3}$$

$$P_{Max} = \sum_{k=0}^{n} c_k \, V_{opt} \, k \tag{4}$$

Where: *n* is the degree of polynomial and are these constants of polynomial and *dopt* is the optimal duty cycle.The resulting fits of the curves characteristic of GPV using thismethod are displayed by the following

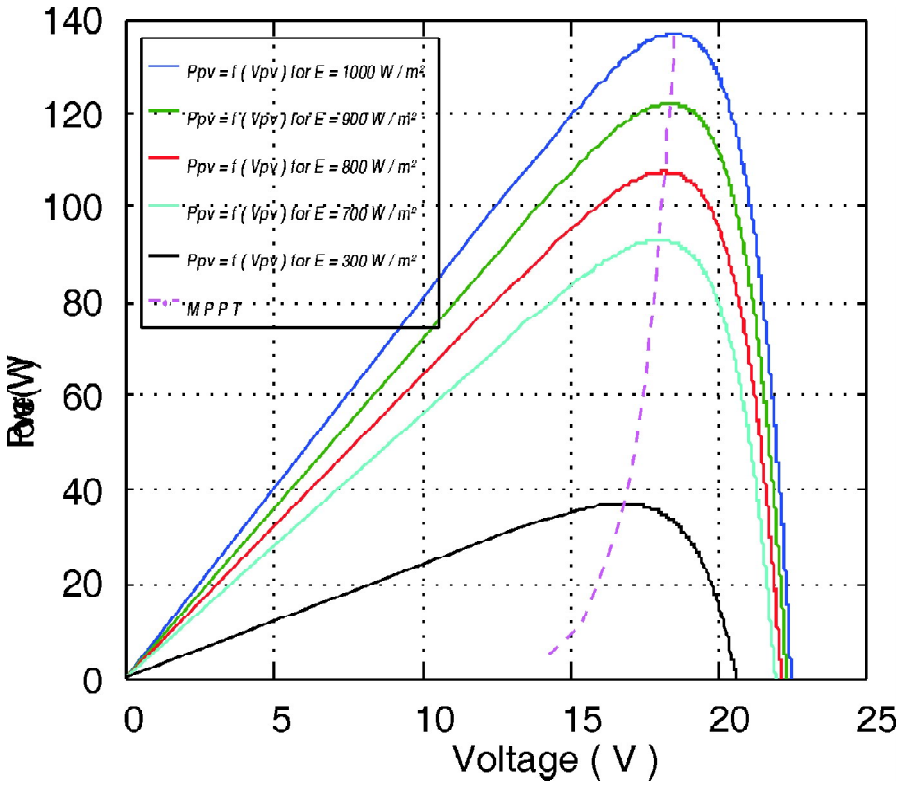

Figure 5: Trajectory of maximum power point of the photovoltaic generator

2.2.2. Lagrange's MPPT Algorithm

For polynomial interpolation techniques, we can find many methods, namely the Vandermonde's method, Lagrange's polynomial method, and the Newton's polynomial method.

We shall examine the Lagrange's method to study the interpolation polynomial whose coefficients are determined by means of the Vandermonde's matrix [10], [11]. We shall concentrate on the bivariate polynomials which have the following general form:

$$P(x,y) = \sum_{i,j} a_{i,j} \, x^i \, y^j \tag{5}$$

Where

$$\forall \, i \; = 0,\ldots\ldots,n \,,$$

The coefficients of the bivariate polynomial $a = (a_j)\ j = 0, ..., n$ are determined by the Vandermande's matrix.

x, y are the variable of this system.

The bivariate polynomial is used for simulation of the system where bothirradiation and temperature variable.The variations of the irradiation and temperature during a day are illustrated by Figs. 4 and 6.

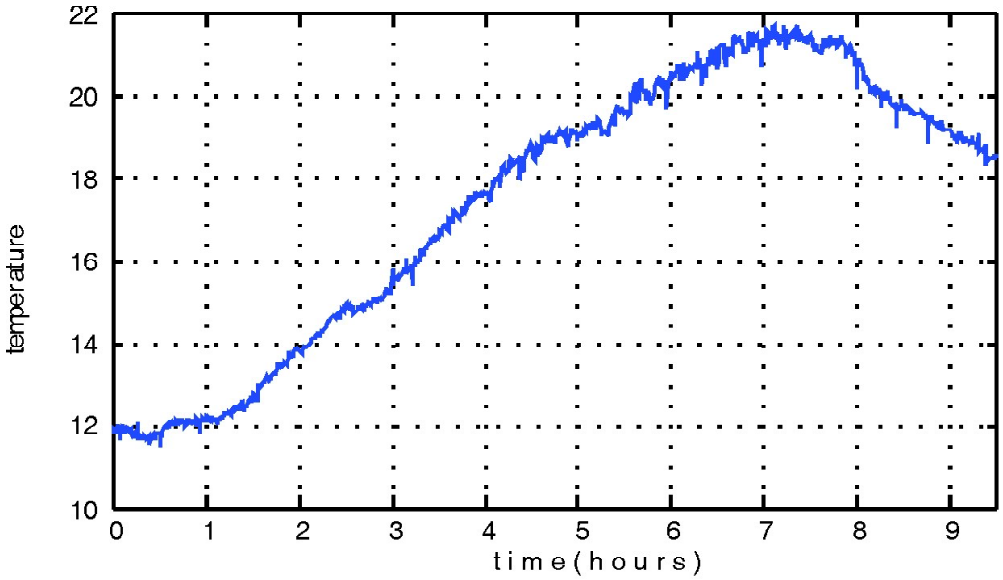

Figure 6: Variation of the temperature during a day in Tunis (Tunisia) on 05 April 2012 [12]

The Matlab software allows us to have the $(n * n)$ Vandermonde's matrix by evaluating the n terms at each of the n points. It also allows determining the coefficients of the polynomial which are written in the following table.

Table 3
Coefficients of the Vandermande's Polynomial Interpolation

$C_1 = 10^{-4}$	$C_2 = -52*10^{-4}$	$C_3 = 845*10^{-4}$
$C_4 = -9*10^{-5}$	$C_5 = 21*10^{-4}$	$C_6 = -1092*10^{-4}$
$C_7 = 6 * 10^{-5}$	$C_8 = 38*10^{-4}$	$C_9 = 6002*10^{-4}$

The resultant polynomial interpolation is described by this following equation:

$$d(E,T) = C_1 * E^2 * T^2 - C_2 * E^2 * T^1 + C_3 * E^2 - C_4 * E * T^2 + C_5 * E * T - C_6 * E + C_7 * T^2 + C_8 * T + C_9 \quad (5)$$

2.3. DC/DC Converter Model

In stand-alone photovoltaic power systems, the output voltage is effectively a constant DC bus due to the slow dynamics of the batteries [8]. Fig.7 presents the topology of the battery storage photovoltaic system

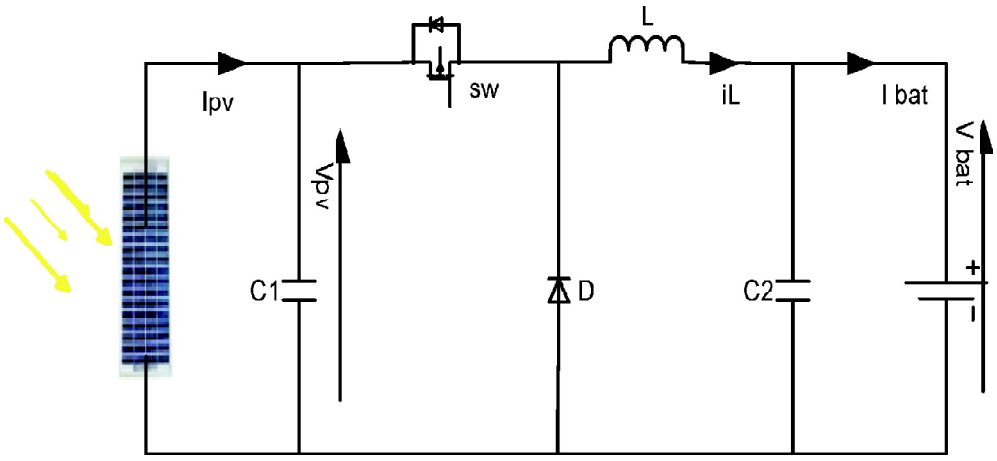

Figure 7: Topology of the energy storage system

The buck converter operates as the power interface between the photovoltaic module and load (battery). Ts and d denotes respectively the switching period and the controlled duty cycle.Fig.8 shows the control signals of the switch SW

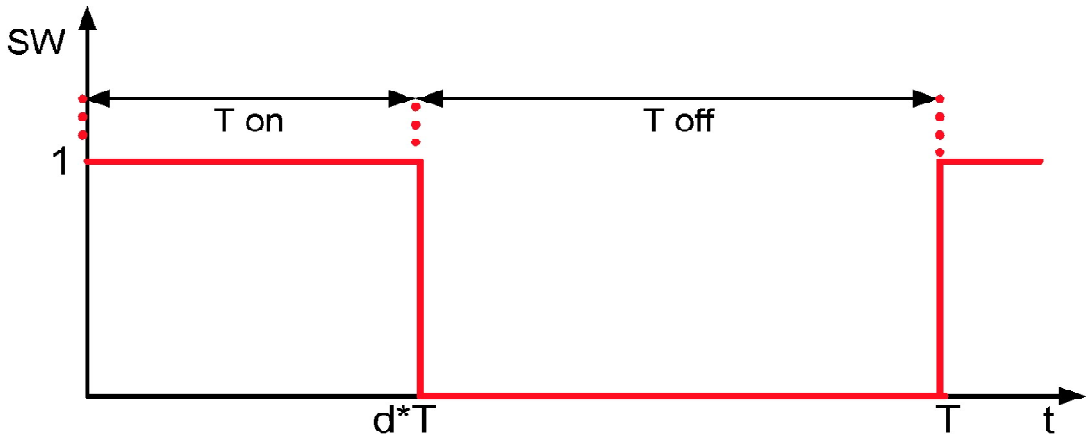

Figure 8: Switch waveform of the converter

There are two stages, first $SW = 1$ and second $SW = 0$

2.3.1. Average Model of DC/DC Converter

To model the converter we choose two state variablesincluding capacitor voltage $Vbat(t)$ and inductor current $iL(t)$. The system state space representation is

$$\dot{x} = A\,x + B\,u$$
$$y = C\,x + D\,u \tag{7}$$

Where: u is the input vector, y is the output vector and x is the status variables vector. $[iL, Vbat]^T$, $u = Vpv$ and $y = V\,bat$

- During the first stage [0 , dT] the equivalent systemtopology is as follows

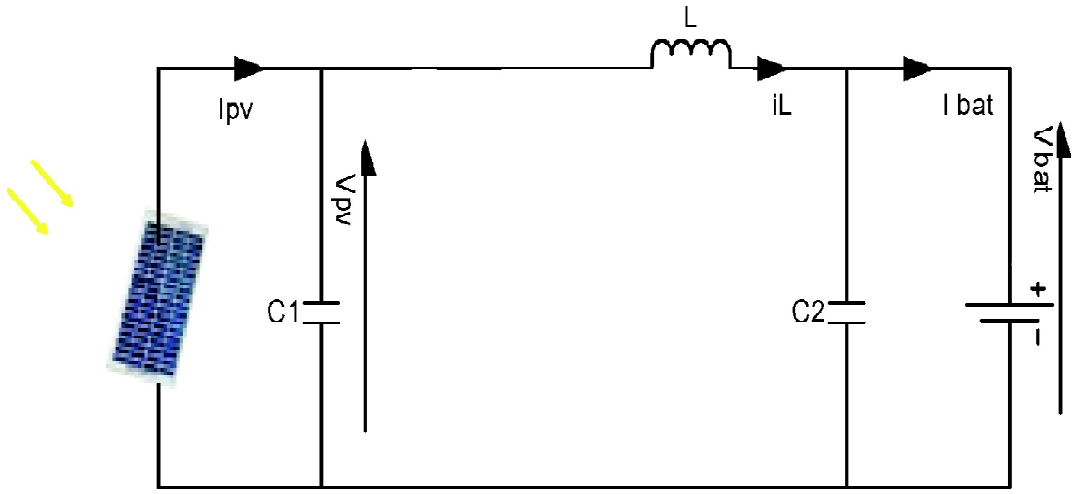

Figure 9: Equivalent circuit (stage 1)

If we apply Kirchhoff's law

$$\frac{d\,i_l}{d\,t} = \frac{V\ pv}{l} - \frac{d}{l} \tag{8}$$

$$\frac{dV\ bat}{d\,t} = \frac{1}{c} * i_l - \frac{1}{c} \tag{9}$$

Spaces of states of the matrix are written as following:

$$\begin{bmatrix} \frac{d\ i_L}{dt} \\ \frac{d\ V\ bat}{d\,t} \end{bmatrix} = \begin{bmatrix} 0 & \frac{-d}{L} \\ \frac{d}{C} & 0 \end{bmatrix} \begin{bmatrix} i_L \\ V\ bat \end{bmatrix} + \begin{bmatrix} \frac{d}{L} & 0 \\ 0 & \frac{-d}{C} \end{bmatrix} \begin{bmatrix} Vpv \\ Ibat \end{bmatrix} \tag{10}$$

In this interval, the state space representation is

$$\begin{aligned} \dot{x}_1 &= A_1 x + B_1 u \\ y_1 &= c_1 x \end{aligned} \tag{11}$$

Where $A_1 = \begin{bmatrix} 0 & -\frac{d}{L} \\ \frac{d}{C} & 0 \end{bmatrix}$, $B_1 = \begin{bmatrix} \frac{d}{L} & 0 \\ 0 & -\frac{d}{C} \end{bmatrix}$ *and* $C_1 = \begin{bmatrix} 0 \\ 1 \end{bmatrix}^T$

- During the second stage [dT, T], the equivalentsystem topology is as follows:

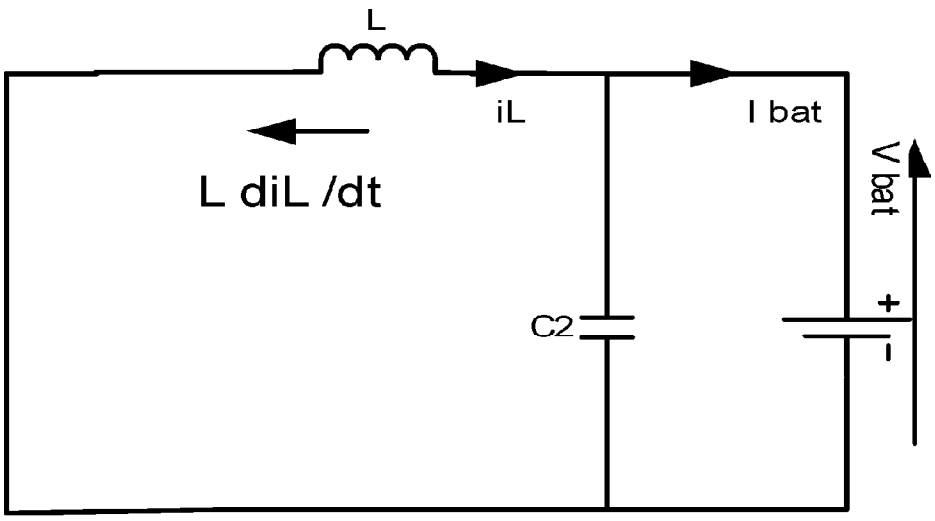

Figure 10: Equivalent circuit (stage 2)

If we apply Kirchhoff's law

$$\frac{d\,i_l}{d\,t} = -\frac{V\,bat}{l} \tag{12}$$

$$I\,bat = \frac{I_{PV}}{d} \tag{13}$$

Spaces of states of the matrix are written as following equation 14.

$$\begin{bmatrix} \frac{d\,i_L}{dt} \\ \frac{dV\,bat}{dt} \end{bmatrix} = \begin{bmatrix} 0 & \frac{d-1}{L} \\ \frac{1-d}{C} & 0 \end{bmatrix} \begin{bmatrix} i_L \\ V\,bat \end{bmatrix} + \begin{bmatrix} 0 & 0 \\ 0 & \frac{d-1}{C} \end{bmatrix} \begin{bmatrix} Vpv \\ I\,bat \end{bmatrix} \tag{14}$$

In the interval, the state space representation is

$$\begin{aligned} \dot{x} &= A_2 x + B_2 u \\ y &= C_2 x \end{aligned} \tag{15}$$

Where

$$A_2 = \begin{bmatrix} 0 & \frac{d-1}{L} \\ \frac{1-d}{C} & 0 \end{bmatrix}, B_2 = \begin{bmatrix} 0 & 0 \\ 0 & \frac{d-1}{C} \end{bmatrix} \text{ and } C_2 = \begin{bmatrix} 0 \\ 1 \end{bmatrix}^T$$

Finally, the averaged model state equation obtained is the following

$$\dot{x} = Ax + Bu$$
$$y = Cx \tag{16}$$

Where

$$A = dA_1 + (1-d)A_2 = \begin{bmatrix} 0 & \frac{-d^2 + d - 1}{L} \\ \frac{d^2 - d + 1}{L} & 0 \end{bmatrix}, \quad B = dB_1 + (1-d)B_2 = \begin{bmatrix} \frac{d^2}{L} & 0 \\ 0 & \frac{d}{C} \end{bmatrix} \text{ and}$$

$$C = dC_1 + (1-d)C_2 = \begin{bmatrix} 0 \\ 1 \end{bmatrix}^T$$

2.3.2. Dynamic Reponse of the DC/DC Converteraverage

The elaborated model is simulated by Matab/Simulink with the following parameters

Table 4
Simulations Parametrs

Vpv_{opt} = 17,6V For E = 1000W / m2 and T = 298 °K
Vbat = 12V, C = 55 µF, L = 120 µH, D = 0.68

Fig. 11 Shows the dynamic behaviour of the converter when a change of illumination occurs. We notice that the output voltage of the DC/DC converter requires 10 seconds to stabilize. This result allows us to discern that this converter presents a high-precision.

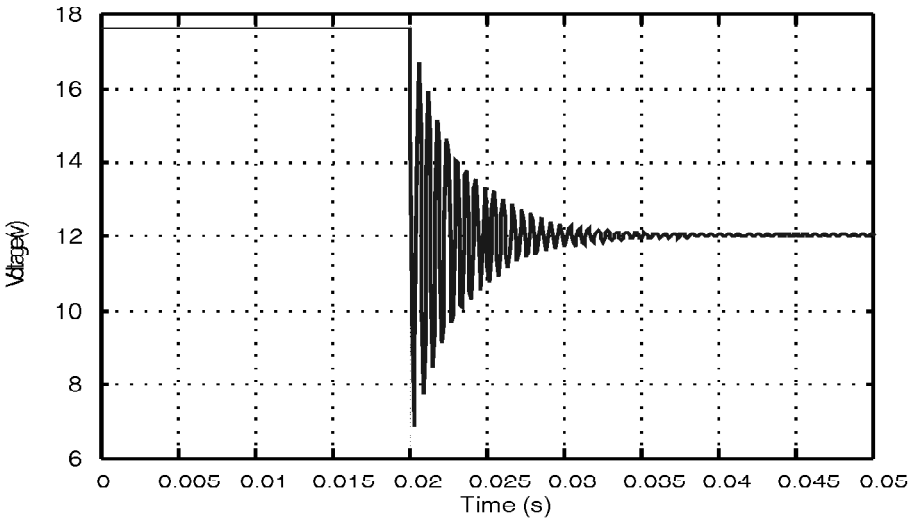

Figure 11: Temporal response of the average back converter

2.4. Battery Model

A parameterized dynamic model used to represent most popular type of rechargeable battery [6]. The equivalent circuit of the battery is shown below

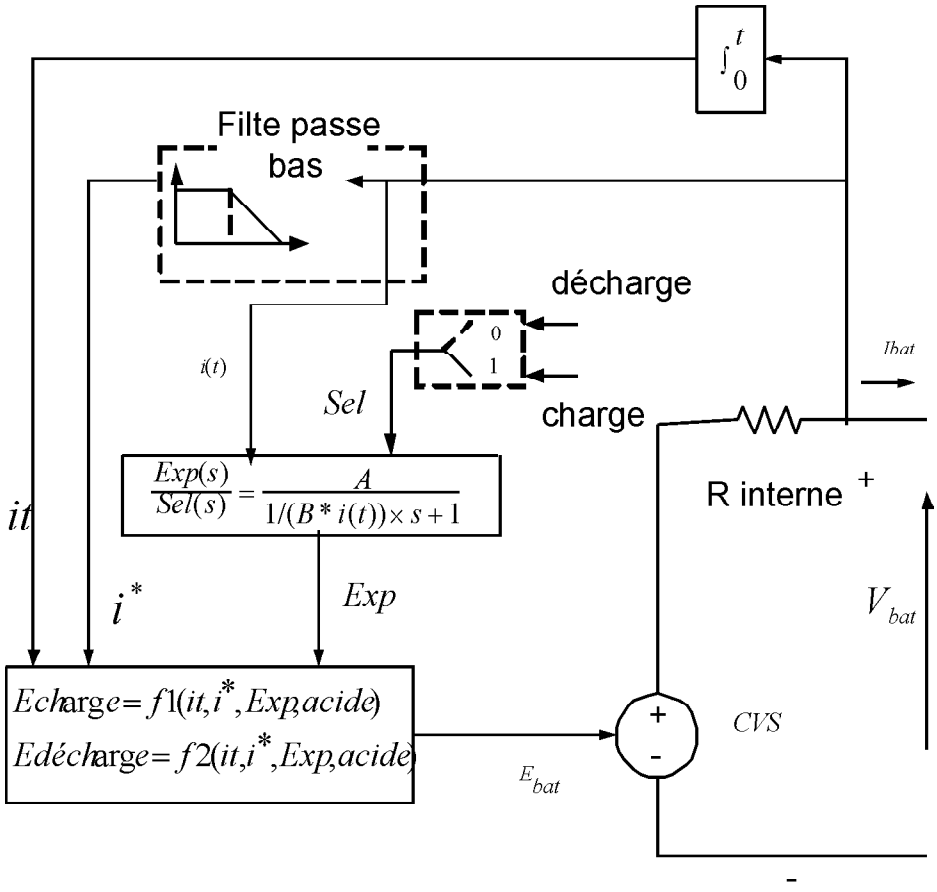

Figure 12: Battery model lead acid type

The relationship governing the charging and discharging of this battery are given by next equations

- Discharge Model $(i^* \succ 0)$

$$f_1(it,\ i^*,\ i,\ Exp) = E_0 - K\frac{Q}{Q-it}\ i^* - K\frac{Q}{Q-it}\ it + Laplace^{-1}\left[\frac{Exp\ (s)}{Sel\ (s)} \times 0\right] \quad (17)$$

- Charge Model $(i^* \prec 0)$

$$f_2(it, i^*, i, Exp) = E_0 - K\frac{Q}{it + 0{,}1 \times Q}\ i^* - K\frac{Q}{Q-it}\ it + Laplace^{-1}\left[\frac{Exp\ (s)}{Sel\ (s)} \times \frac{1}{s}\right] \quad (18)$$

Where:

E_{bat} = Nonlinear voltage (V), E_0 = Constant voltage (V)

$Exp(s)$ = Exponential zone dynamics (V)

$Sel(s)$ = Represents the battery mode. $Sel(s)=0$ during battery discharge, $Sel(s)=1$ during battery charging

K = Polarization constant (Ah^{-1}) or Polarization resistance $(O\,hms)$

i^* = Low frequency current dynamics (A), i = Battery current (A), it = Extracted capacity (Ah)

Q = Maximum battery capacity (Ah)

A = Exponential voltage (V)

B = Exponential capacity (Ah^{-1})

The parameters of the equivalent circuit can be modified to represent a particular battery type, based on its discharge characteristics. A typical discharge curve is composed of three sections, as shown in the fig.13. The first section represents the exponential voltage drop when the battery is charged. Depending on the battery type, this area is more or less wide.The second section represents the charge that can be extracted from the battery until the voltage drops below the battery nominal voltage. The third section represents the total discharge of the battery, when the voltage drops rapidly.

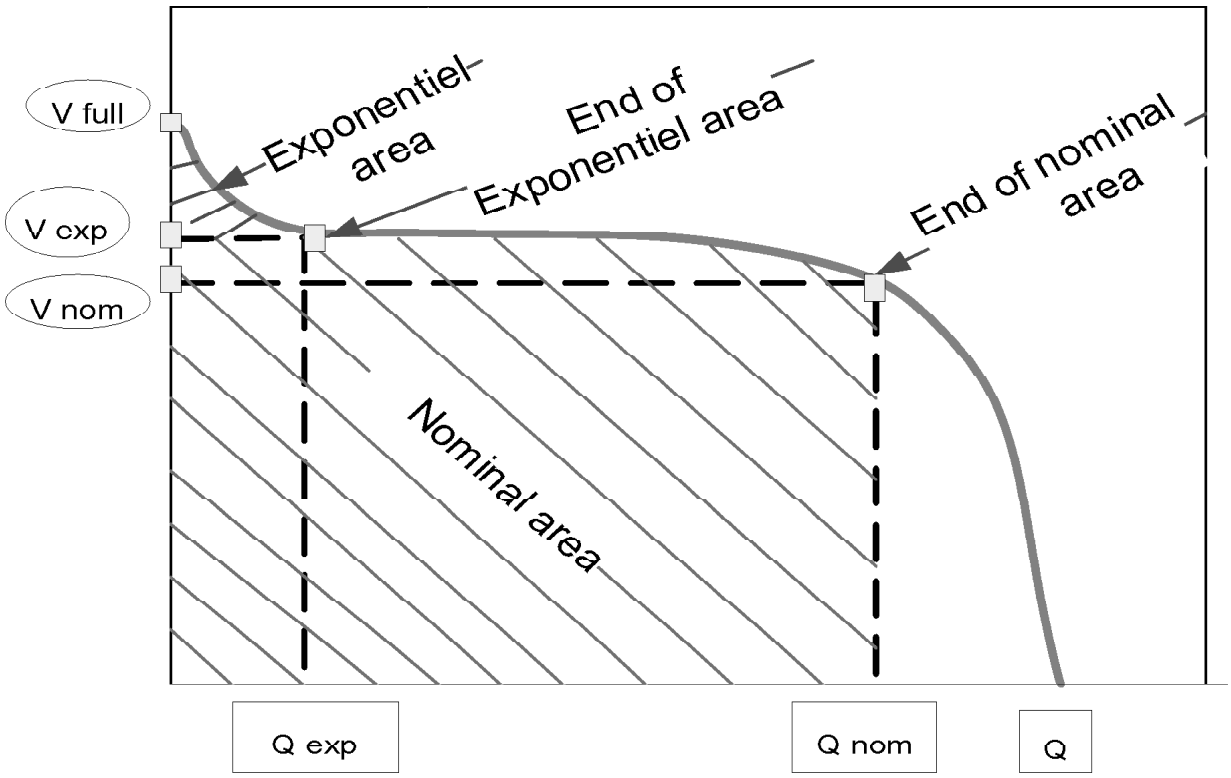

Figure 13: Typical discharge characteristic

In our case, we used a lead acid battery whose characteristics are illustrated in the following table

Table 5
Battery Parameters

Nominal voltage battery	$V_n = 12\ V$
Nominal capacity battery	$Q_{\max} = 100\ Ah$
Full charged voltage	$Vfull = 13\ V$
internal resistance battery	$r_n = 0{,}0012\ \Omega$

3. SIMULATIONS RESULTS AND DISCUTION

The aim of these simulations is to investigate the efficiency of our model of converter and the effectiveness MPPT method used to the energy-storage photovoltaic system under variable climatic condition along a day. These simulations are done with following data:

- The irradiation experimental measurement, illustrated in Fig.4 is processed with Matlab software under of samples 15 seconds.
- The temperature experimental measurement, illustrated in Fig.6 is processed with Matlab software under of samples 15 seconds

The simulations results illustrated by Figs. 14, 15, 16 and 17 show that: the duty cycle change which control the converter is proportional the change of solar irradiation (at constant temperature).This converter operate at maximum power points, it presents no power loss as shown in Fig. 15. The maximum power generated by the panel is transferred to the battery. The difference which appeared in Fig. 16 is due to the voltage drop caused by the internal resistance of the load. The changes of battery characteristics (I_{bat}, V_{bat}, SOC) and the same of GPV (P_{PV}) proportionally with the variable illumination shows the efficiency and the performance of this average model of the DC/DC converter and also the least squares method used. As an addition, the simulated data was analyzed to calculate the efficiency of converter, which was calculated based on energy extracted by converter and the energy stored in the battery. It was evaluated at 91%.

Ended up with a comparative simulation between the preceding case and the one which the temperature and irradiation are simultaneously variable. The resulted is illustrated in figure.18 which shown the diminution of the power du GPV, thus confirming that the variation in temperature is inversely proportional to production of the photovoltaic energy.

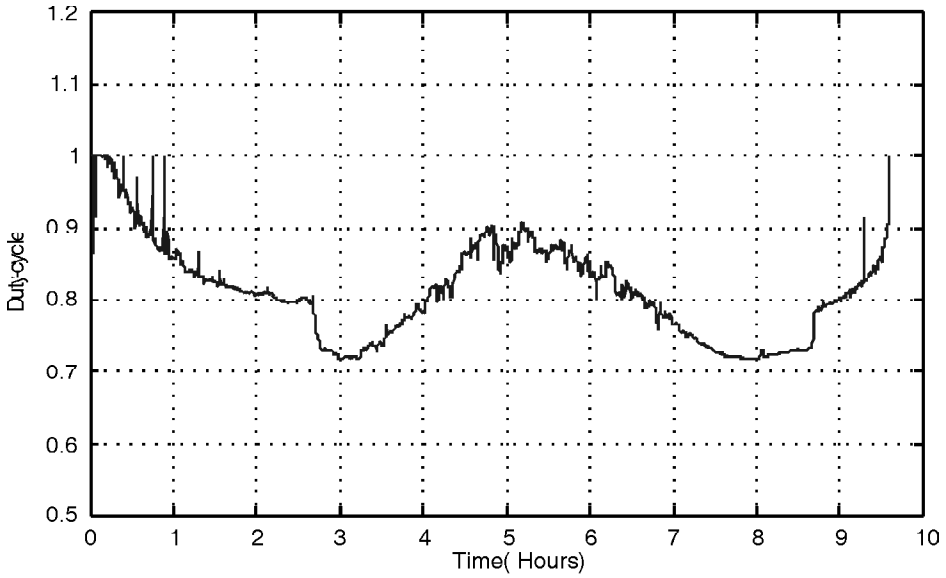

Figure 14: Duty cycle variation

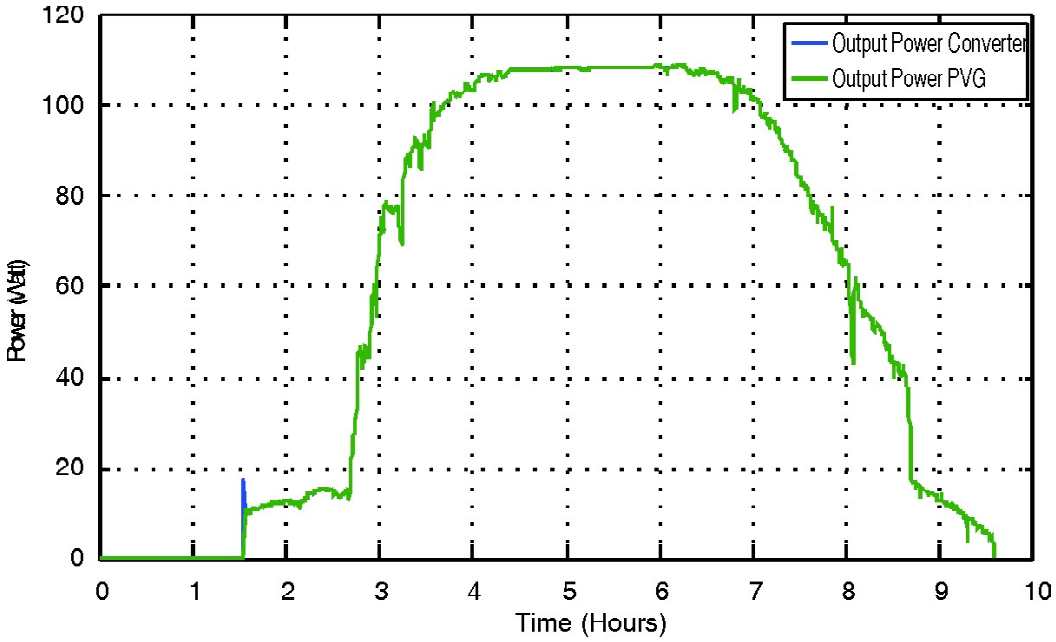

Figure 15: Output power of the converter output of the photovoltaic generator

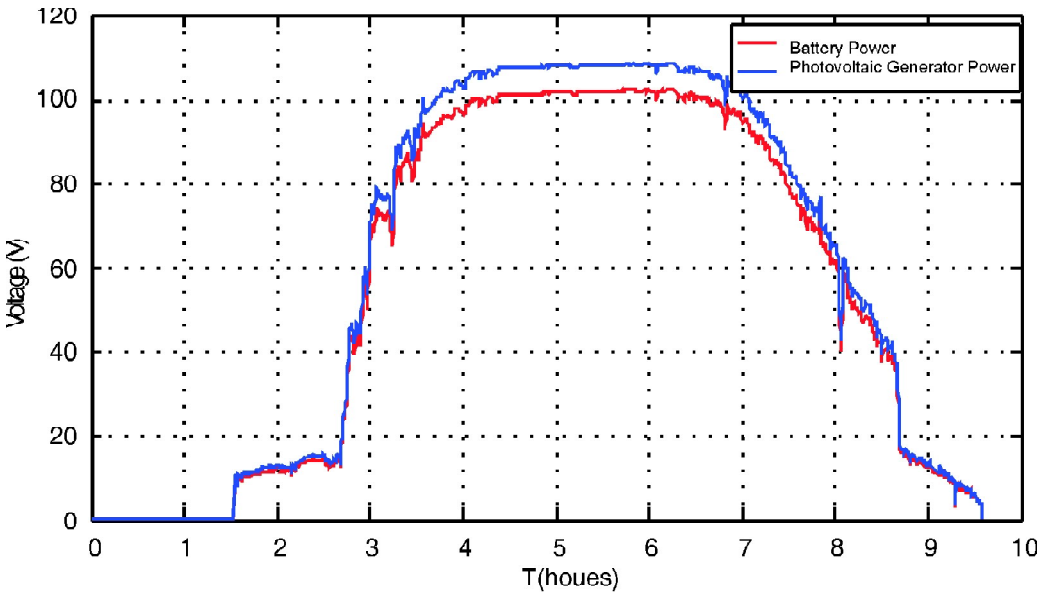

Figure 16: Variations of the GPV power and the power battery as a function time

4. CONCLUSIONS AND FURTHER WORK

Efficient methods for the tracking of maximum power of a photovoltaic generator and a average model of DC/ DC buck converter are designed for a particular application are proposed in this paper.

These MPPT numerical methods are presented for two cases: Firstly the least square numerical method is used for the power transfer between GPV and battery under constant temperature and variable irradiation. Secondly, the Lagrange's method is used for the power transfer under both variables irradiation and temperature. The first

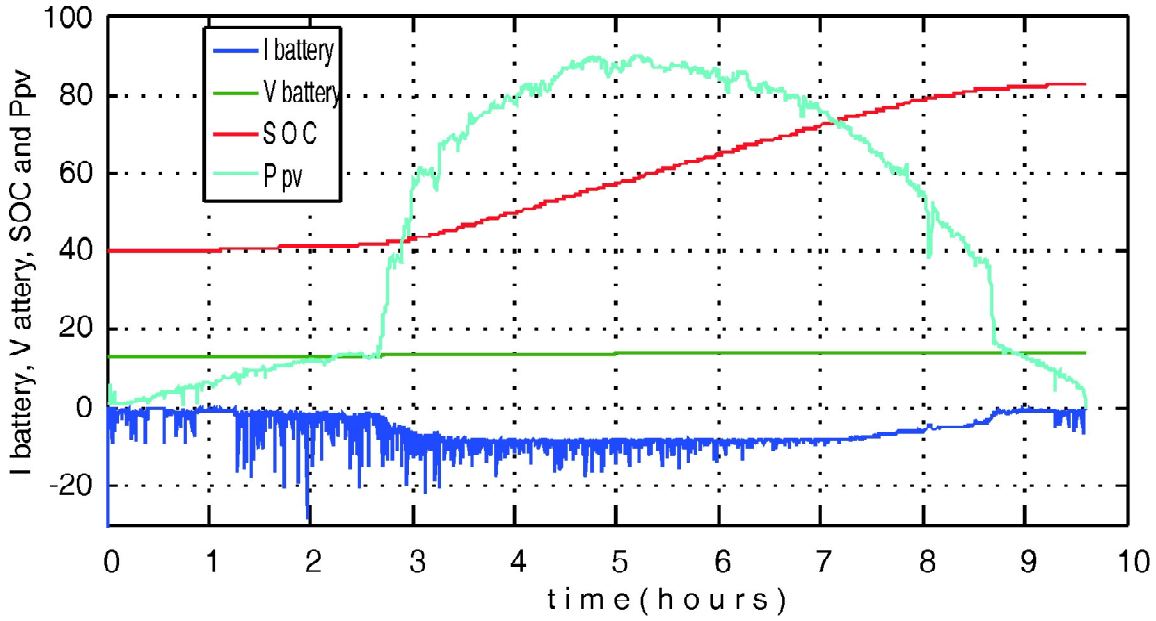

Figure 17: Variations of the characteristics of thebattery and the GPV power

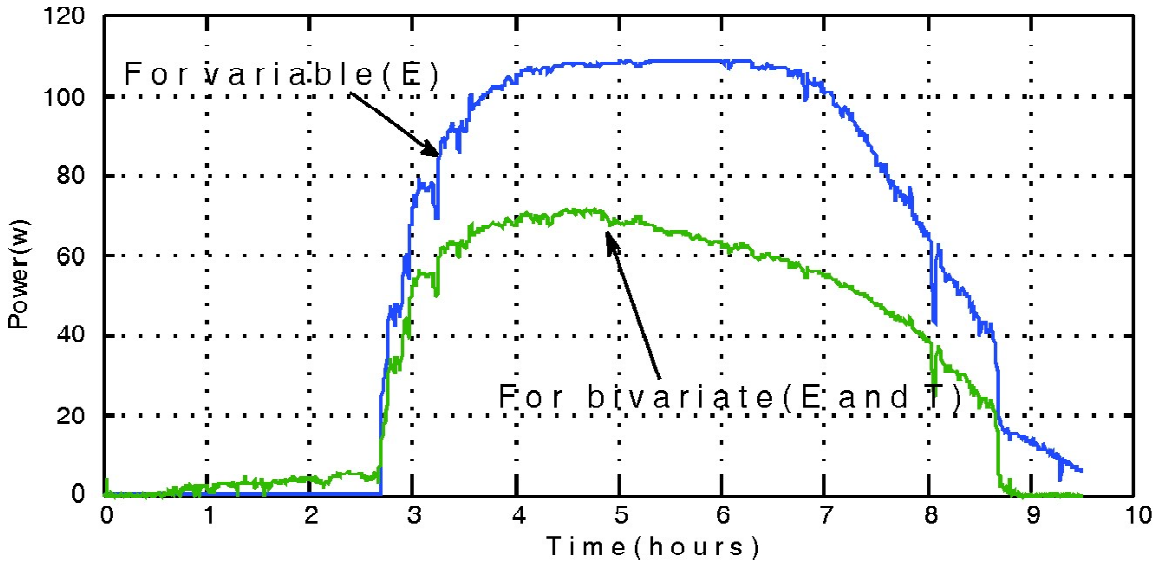

Figure 18: Long term test results of the output power converter and of the $P_{PV} = f(t)$ for (T = 25 C°, E variable) and for bivariate (T, E)

method is used to obtain the best curve fitting that passes through the data points by minimizing errors in the least squares sense. The Lagrange's method is based on the multivariate interpolation polynomial.

In order to investigate these methods, an average model of a DC/DC buck converter is employed. It is based on the state matrices of the battery-storage photovoltaic system.

The goal of these methods is to overcome some of the occlusion problems associated with the precision and the rapidity during the long-term simulations.

These simulation results confirm the high performance of these numerical methods to best optimizationof the energy transfer of this photovoltaic battery-storage system.

REFERENCES

[1] N. Kemali, and F. Bacha , "A maximum power point tracking algorithm applied for photovoltaic water-pumping system," 8th International Symposium on Advanced Electromechanical Motion Systems and Electric Drives, July 1-3, 2009.

[2] Y. Oueslati, A. Sellami, F. Bacha and R. Andoulsi,"Sliding mode control of a photovoltaic gridconnected system", Proceedings of the 2007 International Conference on Electrical EngineeringDesign and Technologies (ICEEDT), November 4-6, 2007, Hammamet, Tunisia.

[3] W. Xiao, N. Ozog, and W.G. Dunford, "Topology Study of Photovoltaic Interface for Maximum Power Point Tracking," *IEEE Transactions on Industrial Electronics*, 54 (3),1696-1704, 2007.

[4] O. Tremblay andL.A. Dessaint, "Experimental validation of a battery dynamic model for EV applications," World Electric Vehicle Journal, 3, 289-298, 2009.

[5] M.E. Ouariachi, T. Mrabti, M.F. Yaden, K. Kassmi and K. Kassmi, "Analysis, optimization and modeling of electrical energies produced by the photovoltaic panels and systems," Revue des Energies Renouvelables, 14 (4), 707-716, 2011.

[6] C. Hua and J.R.Lin, "DSP-based controller application in battery storage of photovoltaic system," Proceedings of theIEEE IECON International Conference, August, 1996.

[7] A.R. Patil, K.D. Atar, A.A. Potdar and R.R. Mudholkar, "Embedded fuzzy module for battery charger control," *International Journal of Advanced Research in Electrical, Electronics and Instrumentation Engineering*, 2 (8), 4072-4078, 2013.

[8] W. Xiao, N. Ozog, and W.G. Dunford, "Topology study of photovoltaic interface for maximum power point tracking," *IEEE Transactions on Industrial Electronics*, 54 (3), 1696-1704, 2007.

M. Amari, J. Ghouili, andF. Bacha , "Average model of a high frequency DC/DC converter for fuelcell application in electrical vehicle," International Conference on Control, Engineering & Information Technology (CEIT'13), Vol.1, pp. 115-121, 2013.

[9] M. Gasca and T. Sauerb , "On the history of multivariate polynomial interpolation," *Journal of Computational and Applied Mathematics*, 122, 23-35, 2000.

[10] M.A. Garcia-March, F. Giménez, F.R.Villatoro, J. Perez,P. Fernandez and C. Sauerb, "Unisolvency for multivariate polynomial interpolation in Coatmelecconfigurations of nodes," *Applied Mathematics and Computation*, 217, 7427-7474, 2011.

[11] K. Echaieb, M. Azaza, A. Chouchaine and A. Mami, "A new control strategyof indoor air temperature in a photovoltaic greenhouse ," The Proceeding of InternationalConference on Soft Computing and Software Engineering 2013 [SCSE'13], San Francisco, CA,U.S.A., March 1-2, 203.

[12] S.Vaidyanathan, "Global chaos synchronization of Duffing double-well chaotic oscillators via integral sliding mode control," *International Journal of ChemTech Research*, 8 (11), 141-151, 2015.

[13] A.T. Azar and S. Vaidyanathan, Chaos Modeling and Control Systems Design, Springer, Berlin, 2015.

[14] S. Vaidyanathan, "A novel 3-D conservative chaotic system with sinusoidal nonlinearity and its adaptive control", *International Journal of Control Theory and Applications*, 9 (1), 115-132, 2016.

[15] S. Vaidyanathan and S. Pakiriswamy, "A five-term 3-D novel conservative chaotic system and its generalized projective synchronization via adaptive control method", *International Journal of Control Theory and Applications*, 9 (1), 61-78, 2016.

[16] V.T. Pham, S. Jafari, C. Volos, A. Giakoumis, S. Vaidyanathan and T. Kapitaniak, "A chaotic system with equilibria located on the rounded square loop and its circuit implementation," *IEEE Transactions on Circuits and Systems-II: Express Briefs*, 63 (9), 2016.

[17] S. Vaidyanathan and S. Sampath, "Anti-synchronisation of identical chaotic systems via novel sliding control and its application to a novel chaotic system," *International Journal of Modelling, Identification and Control*, 27 (1), 3-13, 2017.

[18] S. Vaidyanathan, K. Madhavan and B.A. Idowu, "Backstepping control design for the adaptive stabilization and synchronization of the Pandey jerk chaotic system with unknown parameters," *International Journal of Control Theory and Applications*, 9 (1), 299-319, 2016.

[19] C.K. Volos, D. Prousalis, I.M. Kyprianidis, I. Stouboulos, S. Vaidyanathan and V.T. Pham, "Synchronization and anti-synchronization of coupled Hindmarsh-Rose neuron models," *International Journal of Control Theory and Applications*, 9 (1), 101-114, 2016.

[20] A. Akgul, I. Moroz, I. Pehlivan and S. Vaidyanathan, "A new four-scroll chaotic attractor and its engineering applications," *Optik*, 127 (13), 5491-5499, 2016.